J Mater Sci (2007) 42:3914–3922
DOI 10.1007/s10853-006-0403-2

# Experimental characterization of the stress–strain behaviour of cemented paste backfill in compression

**Mamadou Fall · T. Belem · S. Samb · M. Benzaazoua**

Received: 31 October 2005 / Accepted: 2 May 2006 / Published online: 10 February 2007


**Abstract** It is of great interest for economical and security reasons to understand the compressive properties of underground cemented paste backfill. In this paper, the stress–strain behaviours of cemented paste backfill (CPB) subjected to uniaxial compression and conventional triaxial tests are presented and discussed. The effect of CPB basic components, strength, ageing and confining pressure on the deformation behaviour of CPB are evaluated and discussed. The results show that the stress–strain behaviour of CPB is strongly influenced by the confinement, the age and strength of CPB, and its components. The increase in confining pressure leads to a change in the mode of failure, in the stiffness, and an increase in the strength.

## Introduction

Cemented paste backfill (CPB), a relatively new material, typically consists of a mixture of cement (often 3–7 wt% by weight), tailings and water. During the last decade, CPB has become increasingly popular in underground mining operations around the world. CPB technology is considered superior to conventional slurry backfill method in terms of both economic and environmental benefits [1–7]. Its application is very useful for ground support and to maximize the recovery of ore safely and economically [3, 8, 9].

One of the most important quality criterions for the hardened cemented paste backfill is mechanical stability. Indeed, the paste backfill must remain stable during the extraction of adjacent stopes to ensure the security of the mine workers. The response of a CPB material under load is controlled to a large extent by the stress–strain relation of the constituent materials and the magnitude of stress [9]. Since CPB structures are mostly subjected to compression in their service life, understanding its stress–strain behaviour in compression is of major interest.

However, despite the intensive and increasing use of CPB in underground mining operations, it remains a relatively new technology. Consequently, many fundamental aspects, such as its compressive properties [9–11], are still not very well understood. A solid knowledge of the CPB mechanical behaviour in compression is vital for a rational design, and a safe and efficient analysis of the stability of CPB structures. Therefore, the main objectives of this study are:

- to study the stress–strain properties of cemented paste backfill in compression through an extensive experimental work;
- to evaluate the effect of ageing and confinement pressure on the stress–strain properties;
- to evaluate the influence of the main CPB components (tailings, water and cement) on its stress–strain properties.

M. Fall (✉)
Department of Civil Engineering, University of Ottawa,
161 Colonel By, Ottawa, Ontario, Canada K1N 6N5
e-mail: mfall@eng.uottawa.ca

T. Belem · M. Benzaazoua
University of Quebec in Abitibi-Temiscamingue,
Abitibi-Temiscamingue, Canada

S. Samb
École polytechnique de Lausane, Lausanne, Switzerland

## Experimental program

### Materials used

#### *Tailings materials*

The tailings materials used in this study were collected from three mines in eastern Canada (Mines A, B and C). Mine A is a gold mine, while mines B and C are polymetallic. While the tailings material of Mine A (TA) is originated from highly deformed and altered magmatic rock (sericit schist), the tailings of Mine B (TB) and of Mine C (TC) result from hard magmatic rocks. Thus, from a physical point of view, the tailings TA are relatively soft compared to tailings TB and TC. The main physical and chemical properties of the tailings material are given in Tables 1 and 2, respectively. It can be noted from Table 1 that tailings TB and TC are denser than tailings TA. The sulphur content in tailings from mine A (TA) is lower than 2% and the tailings of mine B (TB) and C (TC) contain, respectively 15% and 26% (by weight) sulphur (Table 2). The sulphur is mainly due to the presence of pyrite ($FeS_2$). To obtain tailings materials with different particles size distributions, the sampled tailings materials were then reprocessed. This step was done by separation of TA by hydrocycloning and sieving (elimination the coarse tailings particles), and of TB and TC by hydrocycloning, creating several grain size classes corresponding to fine (20 μm particles >60 wt%), medium (35–60 wt% of 20 μm particles) and coarse (15–35 wt% of 20 μm particles) tailings.

#### *Binder reagents*

Portland cement type I (PC I) was used as the basic binding agent. It was blended with sulfate resistant Portland cement type V (PC V) or with blast furnace slag (Slag) or Fly Ash. The blending ratios of PC I and PC V were 50/50, while Portland cement and Slag were blended in a ratio of 30/70 or 20/80. Portland cement and Fly Ash were blended in a ratio of 50/50. The main chemical elements in the binders as well as their main physical properties are shown in Table 3.

#### *Waters*

Tap water (TW) with very low sulphate content and sulphated waters (SW) with relatively high sulphate (>1,000 ppm) content were used as basic mixing waters. The use of waters with different sulphate concentration (SW) allowed simulating the effect of sulphate content on the CPB stress–strain behaviour. The waters SW were made by adding specific amount of sulphate concentrate to tap water.

**Table 1** Physical properties of the tailings used

| Element (unit) | Sp ($m^2/g$) | $G_s$ (–) | $D_{10}$ (μm) | $D_{30}$ (μm) | $D_{50}$ (μm) | $D_{60}$ (μm) | $D_{90}$ (μm) | $C_u$ (–) | $C_c$ (–) |
|---|---|---|---|---|---|---|---|---|---|
| TA | 2.40 | 2.86 | 1.78 | 10.51 | 13.89 | 34.99 | 34.99 | 7.79 | 1.36 |
| TB | 1.56 | 3.58 | 3.60 | 13.20 | 28.25 | 39.45 | 145.60 | 10.95 | 1.09 |
| TC | 2.21 | 3.40 | 2.28 | 9.01 | 19.60 | 27.20 | 76.61 | 11.93 | 3.25 |

Sp: specific surface area; $G_s$: specific gravity; $C_u$: Coefficient of uniformity; $C_c$: Coefficient of curvature

**Table 2** Main chemical elements present in the sampled tailings materials[a]

| Element (unit) | Al (wt%) | B (wt%) | Ca (wt%) | Si (wt%) | Fe (wt%) | Mg (wt%) | Mn (wt%) | Na (wt%) | S (wt%) |
|---|---|---|---|---|---|---|---|---|---|
| TA | 5.37 | 0.48 | 5.02 | 20.22 | 8.35 | 3.73 | 0.14 | 2.64 | 1.39 |
| TB | 3.86 | 0.29 | 1.13 | 17.16 | 24.30 | 2.93 | 0.13 | 0.61 | 15.04 |
| TC | 3.52 | 0.11 | 1.01 | 13.09 | 29.47 | 0.29 | 0.01 | 0.91 | 26.08 |

[a] Chemical composition determined by ICP ES analysis

**Table 3** Main physical and chemical characteristics of the binders used[a]

| Element (unit) | Sp ($m^2/g$) | Gs (–) | S (wt%) | Ca (wt%) | Si (wt%) | Al (wt%) | Mg (wt%) | Fe (wt%) | Si/Ca |
|---|---|---|---|---|---|---|---|---|---|
| *Binder type* | | | | | | | | | |
| PC I | 1.32 | 3.15 | 1.5 | 44.9 | 8.4 | 2.4 | 1.6 | 1.9 | 0.2 |
| PC V | 0.97 | 3.19 | 1.2 | 45.5 | 9.3 | 2.0 | 0.9 | 2.7 | 0.2 |
| Slag | 2.16 | 2.84 | 1.21 | 26.6 | 16.9 | 3.9 | 6.9 | 0.5 | 0.6 |
| Fly ash | 2.16 | 2.61 | 1.3 | 13.3 | 15.2 | 9.2 | 2.6 | 4.1 | 1.1 |

[a] Chemical composition determined by ICP ES analysis

### Specimen preparation

CPB specimens having different binder contents, w/c ratios (water-to-cement ratio), and tailings types (gold tailings, polymetallic tailings, tailings with different particle sizes) were prepared. The tailings materials, binders and water were mixed and homogenized in a double spiral mixer for about 7 min to produce the desired CPB mixtures. Then, the consistency of the paste mixtures was measured by slump test according to ASTM C 143-90. The CPB mixes produced were poured into curing cylinders, 10 cm in diameter and 20 cm high. The specimens were then sealed and cured in a humidity chamber maintained at approximately 80% humidity and 23 ± 2 °C. A total of 300 CPB specimens were prepared and cured at different times: 7, 14, 28, 56, 90 and 120 days. Additionally, experimental data from previous studies [5, 6, 9, 10, 12, 13] were used.

### Testing of specimens

#### *Mechanical tests*

Uniaxial compression tests according to ASTM [14] and triaxial compression tests according to ASTM [15] were carried out to evaluate the mechanical properties or behaviour of the prepared CPB samples. For these tests, a computer-controlled mechanical press (MTS 10/GL) of 50 kN capacity was used. The load was applied at a slow rate (1 mm/min). The axial deformations were automatically recorded by an electronic data acquisition system.

#### *Microstructure analysis*

To evaluate the microstructure of CPB subjected to compression and the influence of CPB microstructure on its stress strain properties, the microstructure of selected CPB samples was investigated by Scanning Electron Microscopy (SEM) and by Mercury Intrusion Porosimetry (MIP). The SEM observations were done with a Hitachi®3500-N microscope. MIP measurements were performed using a Micromeretics AutoPore III 9420 mercury porosimeter.

## Results and discussions

### Stress–strain behaviour of CPB in uniaxial compression

Uniaxial compression tests were performed on approximately 80 CPB specimens after different curing times (7, 14, 28, 56, 90, 120 days). Figure 1 shows a set of typical responses of CPB specimens made from different tailings types in uniaxial compression after a curing time of 90 days. It can be seen that regardless of the CPB types (i.e. of the tailings material used), up to stress level of approximately 30–40% of the peak stress the CPB shows an elastic behaviour. Near the peak region, as the stress increases the load deformation curve of CPB shows its first visible non-linear behaviour. Accumulation and localization of microcracks begin to be observed on the tested CPB samples. The strain corresponding to the peak stress depends on the CPB type. The peak strain value is not approximately constant as for normal concrete (~0.2%). In the descending branch the stress level decreases (relatively slowly) with increasing deformations. This phenomenon can be attributed to the propagation of cracks generated in the pre-peak and peak regions. Indeed, as crack opening increases, the stress-bearing capacity decreases. Figure 2a, which represents the SEM micrograph of a CPB specimen loaded up to peak stress, illustrates the microcracks developed in the CPB. Figure 2b shows that no visible microcracks are present in the unloaded CPB. This demonstrates graphically that the initiation and the propagation of cracks is an important mechanism in CPB material response. Figure 1 also shows that the modulus of elasticity of CPB is influenced by the type of tailings material used. CPB made from hard rock tailings (TB, TC) show higher moduli than CPB made from softer tailings. However, the shape of the stress–strain curve is largely influenced by the uniaxial compressive strength (UCS) of CPB. Some typical stress–strain curves plotted in Fig. 3 illustrate the change in shape of the stress–strain curve with increasing CPB's UCS. This figure indicates that the uniaxial stress–strain response of CPB with higher UCS is more linear in the ascending branch than

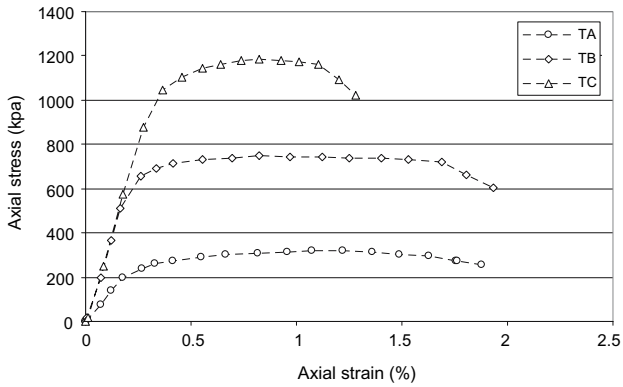


**Fig. 1** Typical stress–strain curves of laboratory CPB samples made from tailings TA, TB, TC (CPB age = 90 days; 3% PCI/Slag; slump: 18 cm)

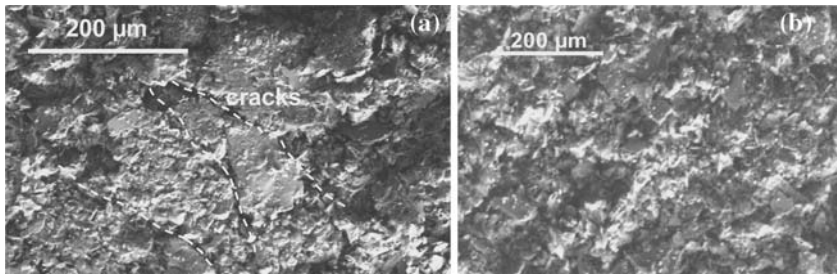


**Fig. 2** SEM images showing (**a**) microcraks in the CPB subjected to uniaxial compression test up to failure and (**b**) no microcracks in the CPB not subjected to uniaxial compression test

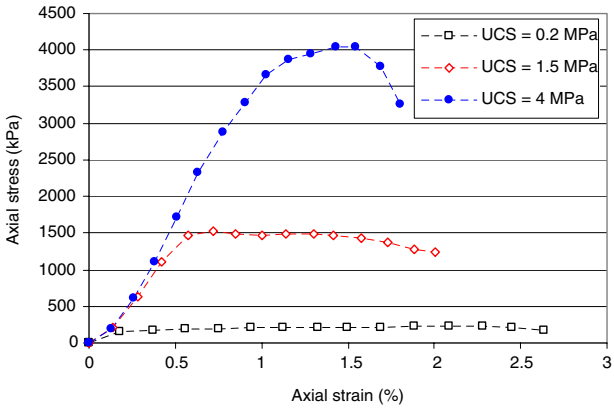


**Fig. 3** Influence of the strength of CPB on the shape of its stress–strain curve (CPB made from tailing TC)

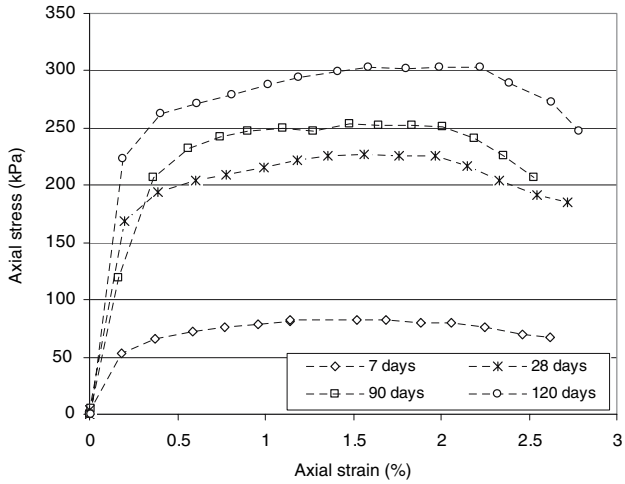


**Fig. 4** Effect of ageing on the stress–strain curve of CPB (CPB made from TA and 3.0% PCI/Slag)

with CPB with lower peak stress, and the descending branch drops off more sharply as the CPB UCS increases. This sharper decrease of the stress–strain curve of CPB with higher UCS can be explained by the following fact: the CPB specimen with higher strength can accumulate a large amount of energy up to the peak stress. This led to a quick propagation of cracks in the failure zone, and consequently stress decreased sharply.

Figure 4 shows the influence of the ageing of CPB on its stress–strain relationship. It indicates that the stress–strain response of CPB is time dependent. Indeed, as expected, when the age of the CPB increases, CPB tends to harden due to the progress of binder hydration. This aging results in the shortening of the peak and post-peak deformation branch, an increase in the peak stress and a gradual increase of the stiffness of the CPB.

## Stress–strain behaviours of CPB in triaxial compression

Triaxial tests were performed on approximately 50 CPB samples cured at different ages. Examples of stress–strain behaviour of CPB subjected to triaxial compression tests are illustrated in Figs. 5 and 6. The peak stress and strain and the stiffness of CPB are affected by the confinement. Visual observation of the CPB samples subjected to triaxial compression and of their stress–strain curves (Figs. 5, 6) indicate that at zero or low confinement pressure, distributed microcracking and several macrocracks are present on CPB samples, and the stress–strain curves show a better-defined and sharper peak (Figs. 5, 6). The increase in

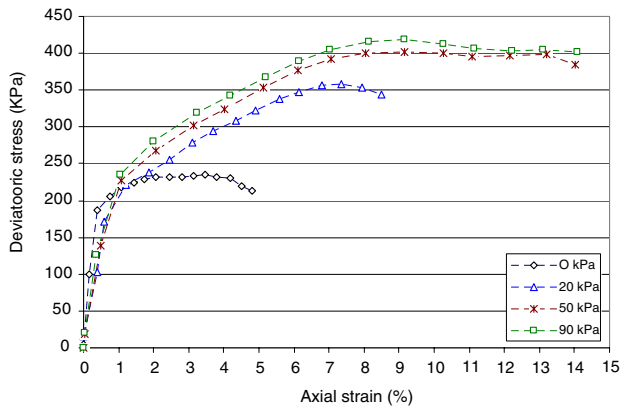


**Fig. 5** Effect of confinement pressure on the stress–strain behaviour of CPB (CPB cured at 28 days, TA, 7% PCI)

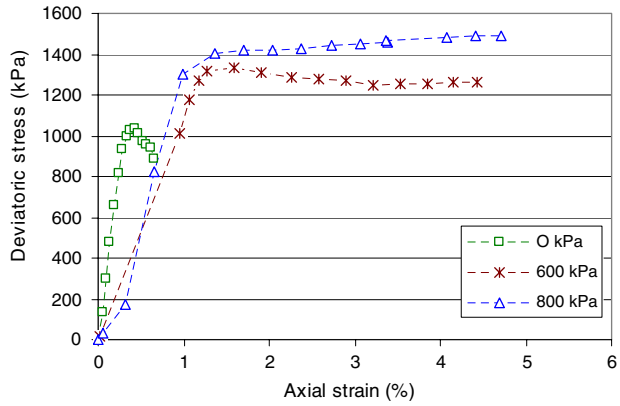


**Fig. 6** Effect of confinement pressure on the stress–strain behaviour of CPB (cured at 91 days, TB, 4.5% PCI/PCV at 50/50)

confinement causes a change in the mode of failure of the CPB at peak stress. Figure 7 shows the effect of confinement ratio $I_c$ (defined as the ratio between the confinement stress $f_l$ and the uniaxial compressive strength) on the compressive strength of CPB specimen having different UCS values. From this figure, it can be seen that, as expected, the deviatioric strength (peak stress) increases with the confinement ratio. For a high confinement ratio, the increase of peak stress with confinement is lower and/or tends to an asymptotical value. However, the influence of confinement on CPB strength is lower with increasing CPB uniaxial compressive strength. This increase of peak stress of CPB with the confinement ratio can be partially attributed to the friction between the fractured surfaces inside the CPB material. Indeed, as shown in the previous section, the development of cracks and their propagation is an important mechanism of the failure of CPB. In the pre-peak region of the stress–strain curve, the growing of cracks in length and width leads to the failure of the CPB. However, with application of confinement pressure, the fractured surfaces tend to be held together, and consequently the resulting increase

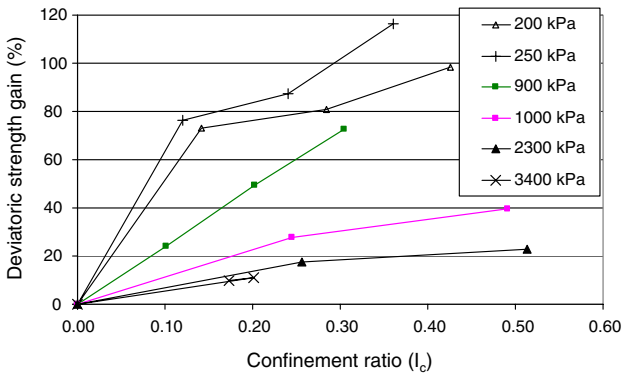


**Fig. 7** Effect of confinement ratio on the strength of CPB having different UCS (UCS indicated in legend)

in friction between the fractured surfaces may continue to support additional axial stress. This friction should increase with the confinement ratio. On the other hand, the constriction of the microstructure of CPB by the confinement pressure should be considered as an additional cause of the increase of the peak strength of the confined CPB.

Figure 8 shows the influence of confinement ratio on the increase in peak strain of some CPB specimens. The ratio ($\varepsilon_{cc}/\varepsilon_c$) between the peak axial strain of confined CPB and that of unconfined CPB is related to the confinement ratio. It can be noted that for a low confinement ratio, the aforementioned ratio increases almost linearly; in other terms, the peak axial strain increases linearly. However, for a high confinement ratio, the slope of the curve representing the increase of $\varepsilon_{cc}/\varepsilon_c$ with confinement ratio decreases.

Figures 5, 6 and 9 demonstrate that the initial modulus of elasticity of the unconfined ($E_{c0}$) and confined ($E_{cc}$) CPB is not similar. Figure 9 shows that increasing the confining pressure decreases first the

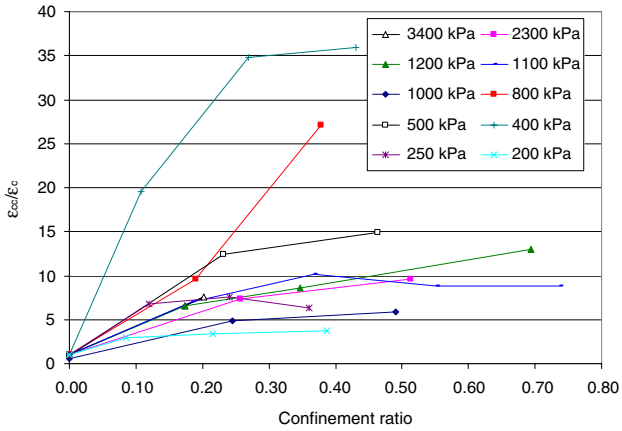


**Fig. 8** Effect of confinement ratio on the increase of peak strain of CPB with different UCS (in legend)

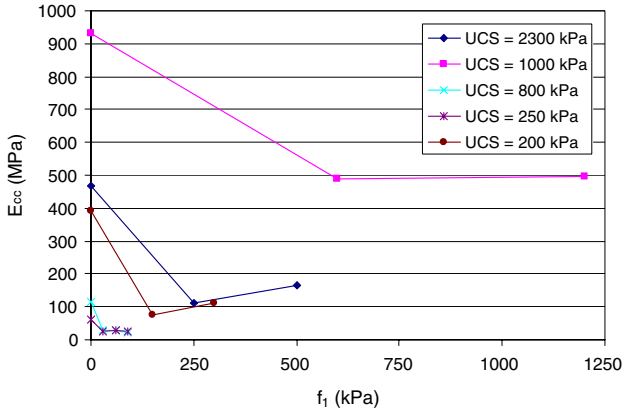


**Fig. 9** Example of curves showing the evolution of the modulus elasticity of CPB with confinement pressure ($f_1$)

elastic modulus, and the rate of this decrease is different for CPB having different UCS. This figure also shows that for a given UCS the effect of confinement on the elasticity modulus of CPB ($E_{cc}$ in MPa) can be predicted by a second degree polynomial in the form (Eq. 3):

$$E_{cc} = A(f_1)^2 + B(f_1) + C \quad (1)$$

where $f_1$ (kPa) is the confinement pressure applied to the CPB sample, A, B, C are coefficients.

At $f_1 = 0$ (i.e. in the case of unconfined situation);

$$C = E_{cc} = E_{c0} \quad (2)$$

where $E_{c0}$ is the initial modulus of elasticity of the unconfined CPB. Upon substituting this boundary condition (Eq. 2) into Eq. 1, Eq. 1 can be rewritten as the following Eq. 3:

$$E_{cc} = A(f_1)^2 + B(f_1) + E_{c0} \quad (3)$$

This Eq. 3 describes the influence of the confinement pressure on the modulus of elasticity of CPB ($E_{cc}$ in MPa); in other terms, it gives the relationship between the elasticity modulus of confined and unconfined CPB. This equation may be useful for modelling the stress–strain behaviour of CPB under compression. Using regression analysis, hypothesis testing at 95% confidence level (generally used in statistics to describe the % confidence attached to a confidence interval, for example 95%) and the experimental data obtained in this study, it was found that for the studied CPBs, $A = 8.55*10^{-4}$; $B = -1.03$.

## Effect of CPB components on its compressive stress–strain properties

Approximately 170 different CPB specimens were used to study the effect of CPB components on its stress–strain properties. Figures 10–13 and 15, 16 illustrate the effect of some main components (binder, water and tailings) of CPB on its stress–strain properties. Figure 10 shows the effect of binder content on the stress–strain properties of CPB. As for a normal concrete, the stress strain properties (e.g. stress–strain curve, peak stress and strain, modulus of elasticity) of CPB are significantly influenced by the binder proportion. It shows clearly that the peak stress and Young's modulus of CPB increases with the binder content (Fig. 10b). The peak stress increases almost linearly with the cement content. The increase in binder content leads to a change in the mode of failure at peak stress. It can be seen that at high binder content, the response exhibits a more defined peak and subsequent softening, whereas for the low binder content it will be more ductile and lead to horizontal plateaus. These results are similar to the results obtained by [10]. This difference in stress-strain behaviour of CPB with different binder contents can be attributed to the fact that higher binder content leads to the formation of more cement hydration products and thus to stronger hardened CPB [16–20].

Figure 11 points out that not only the binder content but also the binder type significantly affects the stress–strain behaviour of CPB. From this figure, it can be observed that CPB samples containing Slag show higher strength and modulus of elasticity than those containing Fly Ash or only Portland cement. Their strain at peak stress is also greater. This influence of the mineral admixture (Slag) on the stress–strain behaviour of CPBs can be attributed to their filler and pozzolanic effect [16, 21–24]. Indeed, it is well known [16, 21–24] that the mineral admixture (Slag) improves the microstructure and strength of cemented material in two ways. First, its small particle size results in a filler effect by which the fine Slag grains bridge the spaces between cement particles and spaces between cement particles and tailings grains. This bridging effect leads to denser packing within the cement matrix. Second, the Slag mineral admixture reacts with calcium hydroxide (CH) formed during the hydration of the Portland cement to produce secondary calcium silicate hydrate (C–S–H) (in addition to the C–S–H

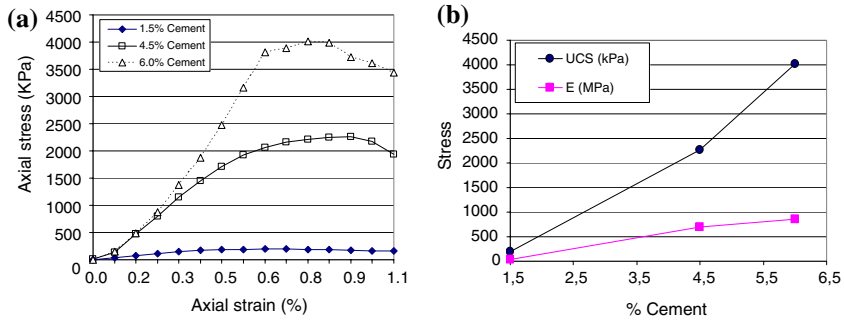


**Fig. 10** Effect of binder proportion on (**a**) the stress–strain behaviour, (**b**) the peak stress (UCS) and young's modulus (E) of 28-day-old CPB (PCI cement, TC used, slump: 18 cm)

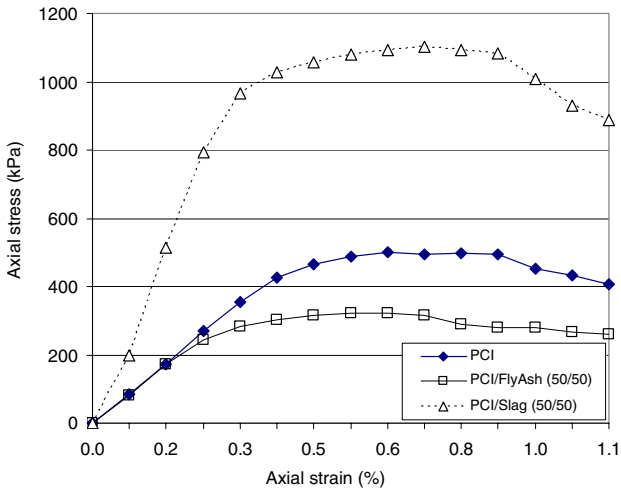


**Fig. 11** Effect of binder type on the stress–strain behaviour of 28-day-old CPB (4.5% cement, TC used)

formed from the hydration of Portland cement) that has a greater volume than the original solid reactants. Considering the fact that according to ref. [16] C–S–H is generally accepted as being the major load-bearing phase in cement paste, it is evident that increasing the C–S–H content in the cement matrix will lead to a higher bond strength between tailings particles and the cement matrix, and consequently to a higher CPB strength and modulus of elasticity.

From Fig. 12 it can be observed that at given strain CPBs with lower w/c ratios can sustain more stress both before and after the peak stress load (Fig. 12a) and they have higher Young's modulus (less deformable) than the CPB samples with higher w/c ratio (Fig. 12b). Generally, the results obtained show that the peak stress and Young's modulus of CPB increase approximately linearly with deacreasing w/c ratio. These observations can be explained by the effect of w/c ratio on the overall porosity of the CPB. The lower water content (a lower w/c ratio) causes a decrease in the total porosity of CPB samples [6], because the volume of capillary voids in a cement paste is essentially determined by the quantity of water mixed with the cement at the start of hydration and the degree of cement hydration [16]. Therefore, for a given curing time or degree of hydration, CPBs with a lower w/c ratio show lower total porosity values. This decreasing porosity or void spaces then causes an increase in CPB strength and modulus of elasticity. The decrease in strength with an increase in the overall porosity of CPBs is consistent with the well-known fact that in solids there is an inverse relationship between porosity and strength.

Figure 13a and b underline that the tailings particle size plays a non-negligible role in the mechanical behaviour of CPB. The peak stress and modulus of elasticity increase with decreasing fineness of the tailings material (Fig. 13b), as observed by [25]. The increase is higher for the CPB made from tailings containing more than 50% fine particles than for CPB made from coaser tailings. This improvement of the mechanical behaviour of the CPB with a decrease of the fines particles proportion (up to 30% fines particles)

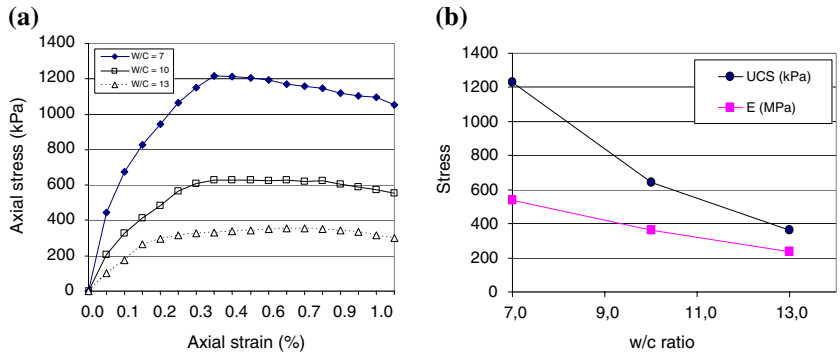


**Fig. 12** Effect of w/c ratio on (**a**) the stress strain behaviour, (**b**) the peak stress (UCS) and young's modulus (E) of 28-day-old CPB (4.5% PCI/Slag: 20/80; TC used)

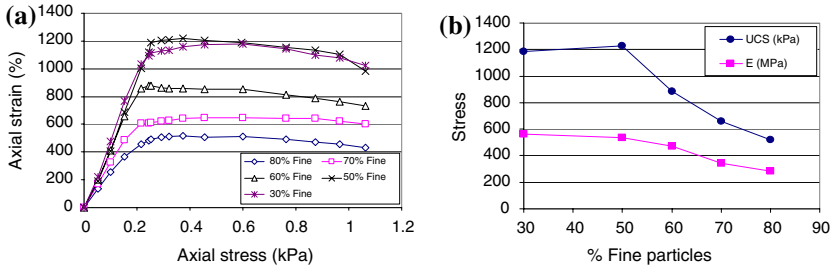


**Fig. 13** Effect of tailings fineness on (**a**) the stress–strain behaviour, (**b**) the peak stress (UCS) and young's modulus (E) of CPB (28 days curing; 4.5% PCI/Slag: 20/80; TC used; slump = 18 cm)

can be attributed to the fact that decreasing of the tailings fineness decreases the water demand of the fresh CPB (lower w/c ratio), giving the hardened CPB a lower packing density and consequently a lower porosity. The results (Fig. 14) of MIP tests on 28-day-old CPB specimen made with the same tailings material but with different grain size support this analysis. It can be seen that the porosity decreases with the tailings fineness, leading to a higher densification of the cement paste and interfaces between tailings particles and cement matrix, the result being an increase of the bonding strength at these interfaces. The consequence is the reduction of the formation of microcracks at the pre-peak region and the retardation of the opening of macrocracks at the beginning of the peak region. In consequence, the peak stress of the CPB increases. Another mechanism contributes to the decrease of CPB strength with tailings fineness. The finer particles increase the specific surface of the tailings materials and thus increase the surface area that must be cemented, since the cement coats the surface of the tailings particles [16]. This effect also contributes to a strength decrease of the CPB with increasing tailings fineness.

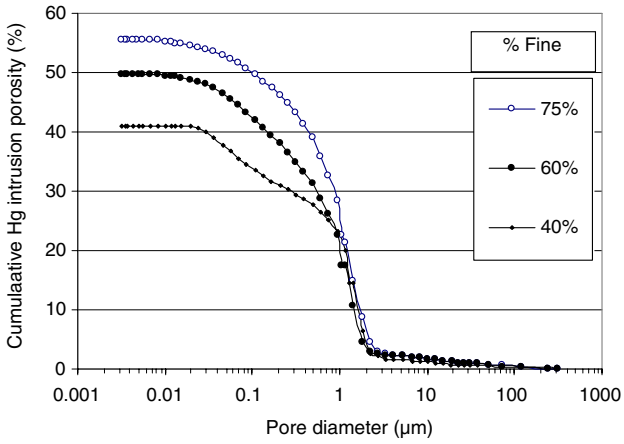


**Fig. 14** Hg Porosity for different tailings fineness (CPB made from 4.5% PCI/Slag)

Figure 15a and b shows that a high sulphate content significantly affects the mechanical behaviour of CPB. At early age (28 days curing time), the higher the sulphate content, the lower the peak stress and the Young's modulus (Fig. 15b), a result of the inhibition of the cement hydration reactions by the sulphate [12, 26]. After longer curing times, the strain–stress curves are altered by the presence of sulphates (Fig. 16a, b). High sulphate content reduces the peak stress of the CPB, leads to flatter descending of the stress–strain curve after peak load, and reduces the Young's modulus (chemical damage). For example, from Fig. 16b, it can be observed that from 56 days to 120 days of curing time the modulus of elasticity and the peak stress of the CPB are reduced by approximately 25%. This reduction is attributed to the degradation of the mechanical properties of the cement matrix of the CPB by chemical damage (sulphate attack), possibly caused by the combined effect of the mineral phases (ettringite, gypsum, brucite) resulting from the reactions of sulphate with the cement hydration products. The formation of these

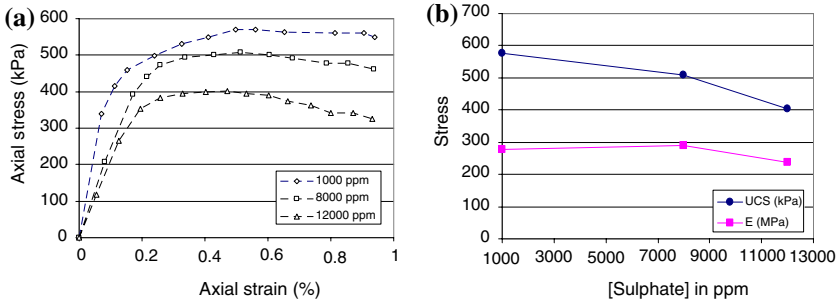


**Fig. 15** Effect of sulphate on stress–strain behaviour, (**b**) peak stress (UCS) and young's modulus (E) of CPB at early age (28 days curing; 4.5% cement; PCI/PCV: 50/50; TB used)

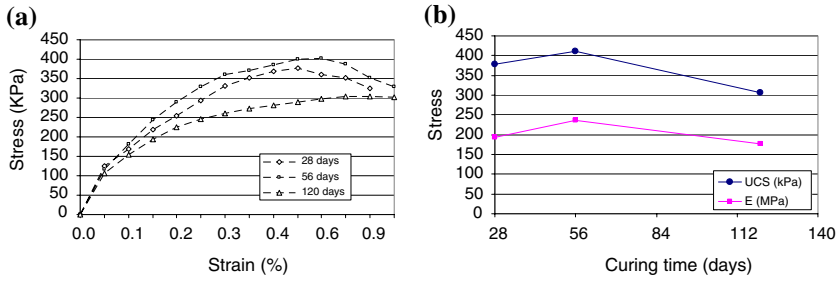


**Fig. 16** Effect of sulphate on the stress–strain behaviour, (**b**) the peak stress (UCS) and young's modulus (E) of CPB (4.5% PCI/PCV: 50/50) (initial sulphate content 5,000 ppm)

mineral phases that have high molar volumes might have produced expansive pressures that have damaged the backfill, and thus caused the loss of strength and stiffness of the CPB material [24, 26].

## Summary and conclusions

The stress–strain behaviour of CPB subjected to compression was examined experimentally. In this experimental work, valuable results were gained regarding the stress–strain behaviour of CPB in compression and the influence of the main components of CPB on its mechanical behaviour, as well as the effect of confinement on the compressive behaviour of CPB. The stress–strain properties of CPB are strongly influenced by the confinement and the cemented paste backfill components. The axial stress–strain behaviours of unconfined and confined CPB are significantly different. The strain corresponding to the maximum CPB stress and the ductility capacity of the CPB generally increase with the confining stress. It was shown that CPBs with lower w/c ratio have higher modulus of elasticity and are more resistant than those with higher w/c ratio. The increase of cement content reduces the ductility of CPB and increases its stiffness. Higher binder contents give the CPB higher strength. CPB made from coarse or medium tailings show higher strength and Young's modulus than those made from fine tailings. The presence of sulphate in the backfill material can lead to the deterioration of the mechanical properties (reduction of the strength and young's modulus) of CPB in long-term through sulphate attack.

**Acknowledgements** The authors would like to acknowledge the IRSST (''Institut de Recherche Robert-Sauvé en santé et en Sécurité du Travail'') and FUQAT for funding a part of this work.

## References

1. Brakebusch FW (1994) Mining Eng 46:1175
2. Landriault D (1995) Proceedings of 97th annual general meeting of CIM. Rock Mechanics and Strata Control Session. Halifax, Nova Scotia, May 14–18, 1995, pp 229–238
3. Hassani F, Archibal J (1998) Mine backfill, CD-Rom. Canadian Institute of Mine, Metallurgy and Petroleum, Canada
4. Grice T (1998) Proceedings of 2nd annual summit, Mine tailings disposal systems, Brisbane, Australian, 14 pp
5. Benzaazoua M, Belem T, Jolette D (2000) Investigation de la stabilité chimique et son impact sur la résistance mécanique des remblais cimentés. Report IRSST, IRSST ed., R-260: 2000, p 158 + Annexes
6. Fall M, Benzaazoua M, Ouellet S (2004) Proceedings 8th international symposia on mining with backfill. In Beijing, China on September 19–21, 2004, pp 193–202
7. Kesimal A, Yilmaz E, Ercikdi B (2004) Cement Concrete Res 34(10):1817
8. Huynh L, Beattie DA, Fornasiero D, Ralston J (2005) Minerals Eng 19(1):28
9. Fall M, Belem T, Benzaazoua M (2005) 58th Canadian Geotechnical and 6th Joint IAH-CNC and CGS Groundwater Specialty Conferences, Saskatoon, Saskatchewan, September, 2005
10. Belem T, Benzaazoua M, Bussière B (2000) Proceedings of 53rd Canadian geotechnical conference, Montreal, October, pp 373–380
11. Rankine RM, Rankine KJ, Sivakugan N, Karunasena W, Bloss ML (2001) Proceedings of the 15th international conference on soil mechanics and geotechnical engineering, Istanbul (Turkey), pp 1241–1244
12. Benzaazoua M, Fall M, Belem T (2003) Minerals Eng 17(2):141
13. Fall M, Benzaazoua M (2003) Proceedings of international conference on tailings & mine waste '03, Colorada, USA; A.A. Balkema, Swets & Zeitlinger, Lisse, ISBN 90 5809 593 2, pp 73–86
14. ASTM C-39-96 Standard Test Method for Compressive Strength of Cylindrical Concrete Specimens 125
15. ASTM D 4767-02 Standard Test Method for Consolidated Undrained Triaxial Compression
16. Mehta PK (1983) First international conference on fly ash, silica fume, slag and other minerals by-products in concrete, ACI Publication SP-79 Volume I, pp 1–46
17. Taylor HFW (1990) Cement chemistry, 3rd edn. Academic Press, Harcourt Brace Jovanovich, Publishers; ISBN 01-12-683900, 475 pp
18. Neville AM (1981) Properties of concrete, 3rd edn. Longman, Essex, England
19. Fall M, Bussière B, Belem T, Benzaazoua M, Samb S (2005) 58th Canadian geotechnical and 6th Joint IAH-CNC and CGS groundwater specialty conferences, Saskatoon, Saskatchewan, September
20. Belem T, Fall M, Aubertin M, Li L (2005) Développement d'une méthode intégrée d'analyse de stabilité des chantiers miniers remblayés, Preliminary report, IRSST project, 28 pp
21. Manmohan D, Mehta PK (1981) Cement Concrete Aggreg 3(1):63
22. Hooton RD (2000) Can J Civil Eng 27:754
23. Abd El.Aziz M, Abd El.Aleem S, Heikal M, El. Didamony H (2005) Cement Concrete Res 35(8):1592
24. Metha PK (1995) In: Skalny J (ed) Materials science of concrete III. American Ceramic Society, pp 105–130
25. Kesimal A, Ercikdi B, Yilmaz E (2003) Minerals Eng 16(10):1009
26. Fall M, Benzaazoua M (2005) Cement Concrete Res 35(2):301